J. Plasma Physics (1997), *vol.* 58, *part* 1, *pp.* 145–161. Printed in the United Kingdom

© 1997 Cambridge University Press

Density profile and current flow in a crossed-field amplifier

D. J. KAUP[1] and GARY E. THOMAS[2]

[1] Institute for Nonlinear Studies, and Departments of Physics and Mathematics, Clarkson University, Potsdam, New York 13699-5815, USA
[2] Communications & Power Industries, 150 Sohier Road, Beverly, Massachusetts 01915, USA

(Received 25 July 1996)

Assuming the averaged (background) electron distribution in a crossed-field device, such as a magnetron or crossed-field amplifier, to be slowly varying between the cathode and the anode, we develop a WKB approximation for the cold-fluid plasma equations of a planar magnetron. In this approximation, we can give general expressions for the solution of linearized, high-frequency oscillations in such a device in terms of two integrals. Assuming also that the high-frequency wave in the slow-wave structure drives the response in the electron plasma, we are then able to show that the current drawn by a crossed-field device will be proportional to the power propagating in the slow-wave structure. Thus the device will operate as a linear amplifier. We also show, in the same approximation, that the averaged electron sheath that forms when the device is operating is independent of the current being drawn. Thus the current will not be limited by the sheath, but only by the ability of the cathode to emit electrons. In the process, we also obtain expressions for the linear growth rate and the value of the quasilinear diffusion coefficient at the diocotron resonance, in terms of parameters of the background electron sheath.

1. Introduction

Much of the earlier theoretical work on magnetrons and crossed-field amplifiers (CFA) had centred on studies of the so-called magnetron instability (Buneman *et al.* 1966; Loveland and Ott 1974; Swegle and Ott 1981; Swegle 1983; Antonsen *et al.* 1985), and also on the stability properties of laminar and kinetic flows (Davidson 1984, 1985*a*; Davidson *et al.* 1984, 1988; Uhm 1992) in crossed-field devices. It now seems that the magnetron instability has little to do with the actual operation of crossed-field devices (Jablonski 1992). It is indeed there (Buneman *et al.* 1966); however, its effect on a crossed-field device is apparently benign. More recently, guiding-centre theory has been used (see Davidson 1984; Riyopoulos 1996; and references therein) to develop a nonlinear model, based on a separation of particle motion into hub motion and spoke motion, as is seen in numerical simulations. Equilibrium studies have been made of electron vortices (Church and Sudan 1995), which are the dominant structures observed in the final stages of amplification. Other recent work by Lau and others (Lau and Chernin 1992; Lau *et al.* 1993; Christensen and Lau 1994) on sheath formation, limiting currents and turbulent microsheaths has revealed

https://doi.org/10.1017/S002237789700576X Published online by Cambridge University Press

important points about sheath evolution. Important numerical studies of relativistic magnetrons (Chan *et al.* 1993) have also revealed that plateau formation can occur at the edge of the sheath, in agreement with the density profile used in the double-box model (Kaup and Thomas 1992*a*). A review of the stability and equilibrium properties of non-neutral electron flows has been given by Davidson *et al.* (1991).

Most recently, there have been experimental studies at Northeastern University (MacGregor *et al.* 1994; Ye *et al.* 1994) on a CFA that contains various diagnostic probes. It is hoped that important experimental information will be gleaned from these experiments, which can give us a better understanding of the important physical effects present in these devices.

In spite of the above theoretical work, the design and manufacture of these devices still remains a well-developed art. The standard operating procedure in the design of a new device is not to use the theory, but rather to use various rules and scaling laws to extrapolate into the desired new parameter regime from the known characteristics of current working devices, and then build a prototype based on these predictions. The device is tested and then the design is modified, based on the results of the tests. This is continued until one has an operational device.

Recent work has shown that the classical Brillouin flow (Brillouin 1945) in such devices can be nonlinearly unstable (Kaup and Thomas 1996) in the presence of high-frequency (RF) waves propagating in the slow-wave structures that these devices contain. As this nonlinear instability evolves, the quasilinear theory (Davidson 1985*b*; Davidson and Tang 1985; Kaup and Thomas 1989) predicts that the electron density will relax to a new profile – one in equilibrium with the propagating RF wave in the slow-wave structure. Thus the presence of a propagating RF mode in the slow-wave structure will drive and distort the original Brillouin flow into a new and different profile. This instability of the Brillouin sheath is not surprising, since earlier kinetic studies in magnetically insulated diodes (Desjarlais and Sudan 1986, 1987), had revealed that stochastic electron motion occurs as the Brillouin limit is approached.

In particular, the well-known classical Brillouin electron-density profile is nonlinearly unstable, with a growth rate inversely proportional to the density gradient at the edge of the sheath (Kaup and Thomas 1996). This instability will occur whenever there is an RF wave present, whose RF frequency ω and RF wave vector k satisfy the wave–particle (diocotron) resonance condition $\omega = kv_d$, where v_d is the drift velocity along the top of the sheath. Thus, as soon as any RF wave that has a resonant frequency enters the device, the classical Brillouin density profile will instantaneously start to change. This rapid transient arises because this nonlinear growth rate is proportional to the density gradient along the edge of the sheath (Kaup and Thomas 1996). Thus, since the classical Brillouin profile has an infinite density gradient at the edge, this growth rate becomes infinite. In an actual device, the density gradient at the edge is not infinite, since there is always at least a small thermal spread in the initial velocities of the electrons, creating a structure along the edge that has a finite, although still large, density gradient (Kaup and Thomas 1988, 1992*b*).

The basis for these results is a careful theoretical analysis of the consequences of the quasilinear theory (Davidson 1985*b*; Kaup and Thomas 1989) when one

https://doi.org/10.1017/S002237789700576X Published online by Cambridge University Press

uses more realistic density profiles, such as the double-box (DB) profile (Kaup and Thomas 1992*a*) or the ramped density profile (Kaup and Thomas 1996). The quasilinear theory is also the natural consequence when one uses a multiple-scale expansion of the cold-fluid equations (Kaup and Thomas 1989).† Many of the consequences and results that we present here were first alluded to in Kaup and Thomas (1989). However, it was only after it had been realized how rapidly this nonlinear growth rate would modify the initial profile that the consequences of the quasilinear theory became sufficiently well appreciated.

The rapidity of this nonlinear growth rate gives us a certain advantage that we exploit in this paper. Let us note that the usual mode of operation of a CFA is in the following manner. First, one imposes the static magnetic field, with no DC (direct-current) voltage applied to the cathode–anode interelectrode spacing. Secondly, the RF signal to be amplified is applied to the input port. Thirdly, and only after the RF signal to be amplified is inside the device, the DC voltage is applied to the cathode–anode interelectrode spacing. Typically, the DC voltage requires hundreds of RF oscillations to ramp up to the maximum of the applied operating voltage. (If the DC voltage were applied before the RF signal was inserted, most CFAs would go into oscillation, like a magnetron, and then would not be able to amplify the input.) This slow rise rate of the applied DC voltage allows us to approximate the initiation of the amplification by a CFA adiabatically. Owing to the rapid nonlinear growth rate of the instability, at any instant, we can consider the applied DC voltage to be a constant, as far as the nonlinear instability is concerned. Thus at each value of the applied DC voltage, we can expect the electron-density profile to have responded to the demands of the nonlinear instability, achieving a stationary state (Kaup and Thomas 1989) for that voltage.

Let us consider what happens as the DC voltage is being turned on, after the RF signal has been injected into the slow-wave structure on the anode. First, at low voltages, there is a very thin sheath. This sheath is too thin to support the diocotron resonance at the RF frequency of the input signal. Thus, at first, there is no quasilinear diffusion, and the sheath remains essentially Brillouin-like. As the DC voltage rises, it finally reaches a value at which the sheath has achieved a sufficient density and thickness to support the diocotron resonance. Now there are electrons at the top of the sheath whose drift velocities v_d can match the phase velocity ω/k of the RF wave.

What happens next can be visualized in the following manner. When the electron drift velocity matches the phase velocity of the RF wave in the slow-wave structure on the anode, in the moving frame of the electron, the electron will see a stationary electric field. Depending on the sign and direction of the seemingly stationary electric field, the initially uniformly distributed electrons can now be bunched and/or accelerated. Some of these electrons will be accelerated, cascading towards the anode. Others will be decelerated, possibly spiralling back into the sheath. In any case, a pattern will develop, possibly quite rapidly, with a basic spatial, moving periodicity of $2\pi/k$. The $2\pi/k$

† In fact, the expansion used in Kaup and Thomas (1989) is stronger than the usual multiple-scale expansion, since most of the separations are based on Fourier components, and such separations are quite insensitive to the strength of any nonlinearity. Within these components, it is only the time scales that could be affected by the strength of the nonlinearity.

https://doi.org/10.1017/S002237789700576X Published online by Cambridge University Press

component of this pattern is the driven RF plasma response. (Of course, there are higher harmonics, but we shall not be interested in them here, since they are presumably non-resonant.) There is another component of the plasma response that we shall need, and it will be defined as follows. If we average the pattern of the total response of the plasma over many wavelengths then we obtain what we shall call the 'background' component. These are the two basic components that we are interested in: the driven RF plasma response and the average plasma background. The actual pattern that develops will be a sum of these two components and all other higher harmonics. However, we shall assume that the higher harmonics are non-resonant and can be ignored. Thus we assume that the major features of the plasma response can be approximated by just the background and the fundamental driven mode.

As noted above, once the drift velocity of the electrons along the top of the sheath becomes large enough to match the phase velocity of the RF wave, these electrons (and all others as well) will start to redistribute themselves according to the quasilinear diffusion process. The initial Brillouin-like electron density profile has become nonlinearly unstable, and thereby rapidly deforms into a 'stationary state' of the quasilinear diffusion process, which will be stable. These stationary states are, in general, quite different from the classical Brillouin density profiles. In particular, they all have finite, negative density gradients, and they all extend from the cathode to the anode, with a non-zero value of the density at the anode (Kaup and Thomas 1989). Furthermore, each state has a non-zero DC current flow where the DC current is proportional to the RF input power. Thus the device acts as a linear amplifier, delivering power to the RF wave, proportional to the input.

To detail these stationary states, we first must obtain solutions for the driven RF plasma response, since this response determines these states. In Sect. 2, we detail the relevant equations for obtaining both the driven RF plasma response and for the quasilinear diffusion process. In Sect. 3, we use the WKB method to construct approximate solutions of the linearized cold-fluid equations, which then give us the general solution for the RF plasma quantities. To construct these solutions, it is necessary to assume some profile for the background density. We shall not specify this profile here, but shall leave it unspecified, except that it must be consistent with what one would expect for the stationary states, as outlined above.

Given the general WKB solution for the driven RF plasma response, we next impose suitable boundary conditions. To fix these, we assume that the cathode is at a fixed potential and that there is some slow-wave structure on the anode, which has an RF wave travelling through it. Imposing these conditions, we then can construct the solution for the driven RF plasma response and also determine the linear growth rate (which is different from the nonlinear growth rate for the background solution) due to the diocotron response, which is done in Sec. 4. With this information, in Sec. 5, we can then construct the quasilinear diffusion coefficient, which determines the DC current flow and the stationary states of the quasilinear diffusion process. We show how these quantities are interrelated, and determine the DC current flow in terms of the electron density at the diocotron resonance. With this, we can then make predictions about the actual DC current that a device will draw. Concluding remarks are made in Sec. 6.

https://doi.org/10.1017/S002237789700576X Published online by Cambridge University Press

2. Basic equations

The geometry and configuration that we shall be using is shown in Fig. 1, which is a diagram of a 'planar magnetron'. A planar geometry is preferred for analytical treatment because of its simplicity. Although actual devices are usually cylindrical, the essential physics is contained in the planar model. At the bottom is the cathode, which is an electron-emitting material. It is located in the (x, z) plane at $y = 0$. We take the ambient magnetic field to be along the negative z axis so that the electron drift velocity will be in the positive x direction. The electron cyclotron frequency is $\Omega = eB_0/mc$, where B_0 is the ambient magnetic field. Next to the cathode is the electron sheath, which extends out for some distance from the cathode. The anode is located at a distance l above the cathode. On the anode is a slow-wave structure, which is simply a waveguide, along which the RF wave will propagate. This slow-wave structure is there (i) to slow down the electromagnetic RF wave, which is moving near the speed of light inside the anode structure and (ii) to select the effective RF (electrostatic) wave vector k that the plasma will see and will respond to.

The basic cold-fluid equations describing this physical system are

$$\partial_t n + \boldsymbol{\nabla} \cdot (\mathbf{v} n) = 0, \tag{1}$$

$$\partial_t \mathbf{v} + (\mathbf{v} \cdot \boldsymbol{\nabla})\, \mathbf{v} - \boldsymbol{\nabla}\phi + \mathbf{v} \times \boldsymbol{\Omega} = 0, \tag{2}$$

$$\nabla^2 \phi = n. \tag{3}$$

In the above equations, the fluid velocity vector is in the (x, y) plane, and all quantities are taken to be independent of the z coordinate. We have also simplified the notation by taking n to be the square of the electron plasma frequency ($n = 4\pi e^2 \rho/m$, where e and m are the electron charge and mass, and ρ is the electron number density) and ϕ to be e/m times the electrostatic potential. We shall use this notation in the remainder of the paper.

We will expand these equations in a perturbation expansion, out to second order, as was done in Kaup and Thomas (1989). We shall first describe the background solution (zeroth order), then the solution for a small RF input signal (first order), and then the equations for the quasilinear (second-order) evolution of the background quantities.

The background equilibrium solution can be obtained from (1)–(3) by assuming all quantities to be independent of x and t and imposing the space-charge-limited current condition at the cathode, which means that the DC electric field is to vanish at the cathode. Thus we have

$$\mathbf{v} = v_0(y)\, \mathbf{x}, \tag{4}$$

$$v_0(y) = \partial_y \phi_0(y)/\Omega, \tag{5}$$

and ϕ_0 is obtained from Poisson's equation

$$\partial_y^2 \phi_0 = n_0, \qquad \phi_0(0) = 0 = \partial_y \phi_0(0), \tag{6}$$

where we have taken the background potential ϕ_0 to be zero at the cathode ($y = 0$) and have imposed the space-charge-limited current condition. Thus, from (6), the solution for $\phi_0(y)$ is determined once $n_0(y)$ is given. At this stage,

https://doi.org/10.1017/S002237789700576X Published online by Cambridge University Press

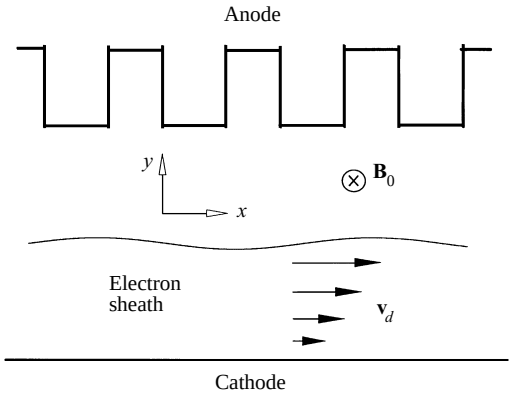


Figure 1. The geometry and configuration of a planar magnetron or CFA. The magnetic field is directed into the paper and the electron drift velocity is to the right. The z axis is perpendicular to the paper, the x axis is parallel to the cathode surface, and the y axis is perpendicular to the cathode.

the background electron-density profile $n_0(y)$ is still arbitrary, except that it must never be negative and it does have to satisfy one integral condition, namely that the potential at the anode, $\phi_0(y = l)$, must equal the applied cathode–anode DC voltage V_0. Also, if the background electron-density profile is to be linearly stable then it is necessary for the density profile to always have a non-positive density gradient (Davidson 1985*b*).

Let us now impose a small RF signal on this background. Linearizing (1)–(3) about this background and taking the perturbed quantities to vary as plane waves, $e^{i(kx-\omega t)}$, we obtain a set of linear ordinary differential equations. We now have a choice of how to reduce these equations. The most common way (Buneman *et al.* 1966) is to eliminate the perturbed particle density and velocities in favour of the perturbed electrostatic potential. However, it is more revealing if we concentrate on the particle velocities instead of the potential. Consequently, we take (Buneman *et al.* 1966; Kaup and Thomas 1989)

$$\partial_y p = Au, \tag{7}$$

$$\partial_y u = Bp, \tag{8}$$

where

$$A = \Omega^2 - \omega_e^2, \tag{9}$$

$$B = \frac{k^2}{A} - \frac{k\partial_y n_0}{\Omega\omega_e A} - \frac{2k^2 n_0 \Delta^2}{\Omega^2 A^2}, \tag{10}$$

$$u = -ikv_{1x}, \tag{11}$$

$$p = Av_{1y}, \tag{12}$$

$$\omega_e = \omega - kv_0, \tag{13}$$

$$\Delta^2 = \Omega^2 - n_0. \tag{14}$$

In the above, ω_e is the frequency of the RF wave as seen by the electron moving at the background drift velocity $v_0(y)$, and Δ is the local orbital oscillating

https://doi.org/10.1017/S002237789700576X Published online by Cambridge University Press

frequency for individual particle orbits (Prasad *et al.* 1987; Kaup and Thomas 1992*b*), which would vanish for a Brillouin flow. In (11) and (12), v_{1x} and v_{1y} are the x and y components of the perturbed velocity fields. The perturbed electrostatic potential ϕ_1, its gradient $\partial_y \phi_1$ and the perturbed electron density n_1 are obtained from p and u as follows (Kaup and Thomas 1989):

$$n_1 = ip\left(\frac{2kn_0^2}{\Omega A^2} - \frac{\partial_y n_0}{A\omega_e}\right), \tag{15}$$

$$\phi_1 = \frac{ip\Delta^2}{Ak\Omega} - \frac{iu\omega_e}{k^2}, \tag{16}$$

$$\partial_y \phi_1 = \frac{i\Omega}{k} u - \frac{i\omega_e}{A} p. \tag{17}$$

The boundary conditions on (7) and (8) follow from the boundary conditions on ϕ_1. At the cathode, which is grounded, the perturbed potential must vanish. Thus $\phi_1(y = 0) = 0$. Then, by (16), we have the ratio of u to p at $y = 0$ determined. This determines the solution up to an overall magnitude. To determine this magnitude, we can match this solution (in the cathode–anode region) to the solution inside the slow-wave structure (Slater 1959). This then will relate u and p to the power being carried by the slow-wave structure.

We remark that these boundary conditions allow v_{1y} to be non-zero at the surface of the cathode. As we shall see from the solution to be obtained later, this value is quite small. Furthermore, we also simply remark that in the presence of an RF signal, the cathode will deliver and absorb electrons according to the demands of the RF electric field at the cathode. Thus the emission and absorption of electrons adjacent to the cathode is to be expected, and is a normal response to the presence of an RF input signal.

The above gives the basic important features of the background solution and the linear theory. Next we consider the second-order, or what has been called the quasilinear, theory. Once we have a small RF signal oscillating in the device as described above, after many oscillations, owing to the nonlinearities in (1)–(3), shifts will start to occur in the background quantities. An analysis of all such shifts was given in Kaup and Thomas (1989), and the results are effectively the same as in the quasilinear theory of Davidson (1985*b*). The main result is that the background potential (and the background density profile) will evolve according to

$$\partial_\tau \partial_y \phi_0 - \Delta^2 C_2 = D\partial_y n_0, \tag{18}$$

where C_2 is a constant of integration, τ is a slow time scale and

$$D = \sum_k \frac{2\gamma p^* p}{\omega_e^* \omega_e A^* A} e^{2\gamma t}, \tag{19}$$

which is the quasilinear diffusion coefficient. In (19), the sum is over all modes and γ is the imaginary part of the RF frequency ω. Furthermore, this is the asymptotic value of D, in the limit that γt is sufficiently large, such that one can ignore the decaying part of the solution. The quasilinear diffusion equation is obtained upon differentiating (18) once. Then, from (6) and (14), we find

$$\partial_\tau n_0 + C_2 \partial_y n_0 = \partial_y (D\partial_y n_0). \tag{20}$$

https://doi.org/10.1017/S002237789700576X Published online by Cambridge University Press

The constant of integration, C_2, is determined by the anode voltage. It can be related to the quasilinear diffusion coefficient and the background density profile by requiring ϕ_0 at the anode to the fixed. Thus, upon integrating (18) from the cathode ($y = 0$) to the anode ($y = l$) and requiring the integral remain constant, we obtain

$$C_2 = \frac{\int_0^l D(-\partial_y n_0)\, dy}{\int_0^l \Delta^2\, dy}. \tag{21}$$

Another significant aspect of C_2 becomes apparent when one considers the particle flux at this order. This was not detailed in Kaup and Thomas (1989), but, using the results presented there, it is a rather simple matter to evaluate this flux. We are only interested in the vertical component, which is $J_y = nv_y$. When this quantity is expanded out, we find that the second-order component is

$$J_{2y} = n_0\, v_{2y}^{(0)} + (\hat{n}_1\, \hat{v}_{1y}^{*} + \text{c.c.}) \tag{22}$$

in the notation of Kaup and Thomas (1989). When this is evaluated, using (18) and (29) from that reference, we find that in the steady state,

$$J_{2y} = C_2\, \Omega^2, \tag{23}$$

which therefore represents a constant, uniform, vertical particle flux, proportional to C_2. If the electron density at the cathode were the Brillouin value of Ω^2 then C_2 would clearly be the vertical velocity of the particle flux at the cathode.

As discussed in Kaup and Thomas (1989), the quasilinear diffusion coefficient will be large (as a function of y) wherever there is diocotron resonance along the edge of a sheath. (When ω is complex, we define the diocotron resonance to be at the value of y where $\Re[\omega_e] = 0$, and where $\Re$ indicating the real part.) Of course, it is necessary that there be an input signal present with modes at these values of the frequencies and wave vectors. As a consequence of this, if there are diocotron resonances present then ϕ_0 and n_0 will rapidly evolve away from their initial (usually Brillouin-like) values and will approach the stationary states of (18). These states are given by (Kaup and Thomas 1989)

$$\Delta^2(y) = \Delta_0^2 \exp\left(C_2 \int_0^y \frac{dy}{D}\right), \tag{24}$$

where Δ_0 is the value of Δ at $y = 0$. From (14), the electron-density profile n_0 of these stationary states can then be determined. Note that these stationary states are only determined by C_2 and the quasilinear diffusion coefficient D. From (24), one can see that the stationary density profile will be monotonically decreasing, with a negative gradient. Furthermore, wherever the quasilinear diffusion coefficient is large, the magnitude of this negative density gradient will be small.

Let us now impose the condition that the electron-density profile must vanish at the anode. This is equivalent to stating that any electron that touches the anode will be immediately absorbed by the anode. This then provides a means for evaluating the unknown constant Δ_0 in (24). Doing so gives

$$\Delta_0^2 = \Omega^2 \exp\left(-C_2 \int_0^l \frac{dy}{D}\right), \tag{25}$$

https://doi.org/10.1017/S002237789700576X Published online by Cambridge University Press

from which it follows that the electron-density profile must be

$$n_0 = \Omega^2\left[1-\exp\left(-C_2\int_y^l \frac{dy}{D}\right)\right]. \tag{26}$$

Thus we have obtained the steady-state density profile in terms of the quasilinear diffusion coefficient and the constant C_2.

These are the basic equations that we shall be using. We shall now proceed to develop a solution for the RF plasma modes, using the WKB approximation, which will be detailed in the next section. In Sec. 4, we shall construct the quasilinear diffusion coefficient and analyse the features of the quasilinear steady states. Lastly, we shall show that the vertical particle flux (current) is proportional to the input power.

3. WKB solution

As detailed by (26), for the steady-state solutions of the quasilinear diffusion equation, the electron density profile is controlled by the exponential of the integral of the inverse of the quasilinear diffusion coefficient. Because of this, we can expect the density profile to be slowly varying in some reasonable sense, since the integral is positive and the exponential is never zero. Certainly, we shall not have any infinitely sharp density gradients as in the Brillouin density profile. Thus we could expect a WKB approximation to work reasonably well with such a background solution.

As detailed in Kaup and Thomas (1996), in the operating parameter regime, typically $\omega < \Omega$, while k is such that somewhere near the top of a Brillouin sheath, $\omega_e = 0$. Considering these facts, we should certainly expect to always have $\omega_e > -\Omega$ everywhere, since ω_e has a negative gradient. Consequently, A then could never have a zero inside the physical region. In this case, we can solve (7) for u,

$$u = \frac{\partial_y p}{A}, \tag{27}$$

and transform (8), using (10), to the second-order ODE

$$A\partial_y\left(\frac{1}{A}\partial_y p\right) - \frac{\partial_y^2 \omega_e}{\omega_e} p - k^2 g p = 0, \tag{28}$$

where

$$g = 1 - \frac{2n_0\Delta^2}{\Omega^2 A} \tag{29}$$

and where the reduction of the second term in (28) was accomplished by use of the identities (5), (6), (10) and (13). Except for the last term and the factors of A inside the first term, this equation would be the Raleigh equation (Drazin and Reid 1981). Many features and references about the Raleigh equation are contained in Drazin and Reid (1981). We shall remark that it is well known that solutions of the Raleigh equation can be very sensitive to the shape of the velocity profile, which, in our case, is the integral of the electron-density profile.

Because of the singularity in the Raleigh equation, it is difficult to construct a full WKB solution for this equation. However, this can be done in a two-step

https://doi.org/10.1017/S002237789700576X Published online by Cambridge University Press

process. First, there is always one solution of the Raleigh equation that is relatively insensitive to the velocity profile. This is the solution that is regular and non-singular near the diocotron resonance at $\omega_e = 0$. Thus this solution can be approximated by a WKB solution. However, the irregular solution is too singular near the diocotron resonance to be represented by a standard WKB approximation. But, as is well known, given one solution of a second-order ODE, one can always construct the second solution by quadrature, using the method of variation of parameters. This we do, and thereby construct the second solution, and obtain approximate solutions of (28).
the form

$$p = \omega_e e^{\Lambda(y)}. \tag{30}$$

Inserting this into (28) gives

$$\left(\lambda + \mu - \frac{A'}{2A}\right)^2 = k^2 g + \mu^2 + \left(\frac{A'}{2A}\right)^2 - \lambda', \tag{31}$$

where the primes indicate differentiation with respect to y and

$$\lambda(y) = \partial_y \Lambda(y), \tag{32}$$

$$\mu(y) = \frac{\partial_y \omega_e}{\omega_e}. \tag{33}$$

Now since $\partial_y \omega_e = -kn_0/\Omega$, it follows that the quantity

$$g + \frac{\mu^2}{k^2} + \left(\frac{A'}{2kA}\right)^2 = \left(1 - \frac{n_0}{A}\right)^2 + \frac{n_0^2}{A\omega_e^2} \tag{34}$$

is positive-definite when A and ω_e are real. Thus, if we ignore the last term in (31), we have as an approximate solution

$$\lambda = \frac{A'}{2A} + \mu\left\{\left[1 + \frac{k^2 g}{\mu^2} + \left(\frac{A'}{2\mu A}\right)^2\right]^{1/2} - 1\right\}, \tag{35}$$

where, since the quantity in the square root is positive-definite, there is no square-root branch cut or singularity. The definition of λ as given by (35) has certain advantages. First, when we are far from the diocotron resonance and/or μ is small, we obtain the standard WKB result for (28). Secondly, when we are near a diocotron resonance, where μ is large owing to ω_e vanishing, λ approaches zero (note that $A' = -2\omega_e' \omega_e$, which also vanishes here). Thus the solution represented by (30) and (35) is the WKB approximation of the regular solution of (28).

The validity of this approximation will depend on how well we can ignore the λ' term in (31). Away from the diocotron resonance where there is no singularity and μ is of order one or smaller, this approximation only requires the various terms to be slowly varying. These we cannot estimate until after we know how rapidly the density profile will vary, but, as we have argued above, we expect it to be slowly varying. On the other hand, for large μ, we are near the resonance and can estimate this term by expanding in powers of $1/\mu$. Doing this for the exact equation, (31), we then find that

$$\lambda' \approx \tfrac{1}{3}k^3(1 - 2n_0) \approx \mu\lambda. \tag{36}$$

https://doi.org/10.1017/S002237789700576X Published online by Cambridge University Press

Thus, for large μ, λ is small and λ' is of order one. We could correct (31) for this, replacing λ' by $\mu\lambda$ instead of zero. However, since λ is small, particularly if n_0 is near $\frac{1}{2}$, and since λ only occurs in an exponential of an integral, the correction would be minor and not important. Thus we shall use the form given by (35) instead. We also note that the value of λ' obtained from (35) is exactly the same as that given by (36), except that the factor of $\frac{1}{3}$ is replaced by $\frac{1}{2}$. Thus (35) does closely approximate the actual solution. Note that this has provided us with a global solution for p, providing that the coefficients are smooth and sufficiently slowly varying, which we should expect to be the case for stationary solutions of the quasilinear diffusion equation.

Let us now uniquely define our solutions of (28). We define the regular solution as

$$p_1 = \frac{\Omega^2}{k}\omega_e\, e^{\Lambda(y)}, \tag{37}$$

where now

$$\Lambda(y) = \int_0^y \lambda(y)\, dy, \tag{38}$$

with $\lambda(y)$ being given by (35). The quantity u_1 follows from (27). It is

$$u_1 = \frac{\lambda+\mu}{A} p_1. \tag{39}$$

The irregular solution of (28) is more difficult to construct. If we attempt to construct it with the other branch of (35), we find that now the λ' term diverges as $\mu \to \infty$ and in general cannot be bounded. The variations in λ are so strong that we would have to solve (31) as a differential equation. However, there is another way to construct the irregular solution. Given that p_1 is an approximate solution, we can always obtain the second solution by quadrature, by simply using the method of variation of parameters. Doing this, we obtain

$$p_2 = \Omega^2\omega_e\, e^{\Lambda(y)} \int_0^y \frac{A(y')}{[\omega_e(y')]^2} e^{-2\Lambda(y')}\, dy' \tag{40}$$

as the second (irregular) solution. The function u_2, from (27), is then

$$u_2 = \frac{\lambda+\mu}{A} p_2 + \frac{\Omega^2}{\omega_e} e^{-\Lambda(y)}. \tag{41}$$

In a sense, (40) is a generalized WKB solution, since it is not in the standard WKB form of a simple exponential. Rather, it has a more complicated structure. This structure has been chosen so as to cause the factor λ to be slowly varying but still able to capture the dominant parts of the solution.

Lastly, we need to construct the solutions for the potential and its gradient, since the boundary conditions are in terms of these quantities. From (16) and (17), we obtain

$$\phi_1 = \frac{i}{k^2 A}\left(\frac{\Delta^2}{\Omega} - \omega_e \frac{\lambda+\mu}{k}\right) h_1\, e^{\Lambda}\Omega^2\omega_e + h_2\, kp_2) - ih_2 \frac{\Omega^2}{k^2} e^{-\Lambda}, \tag{42}$$

$$\partial_y \phi_1 = \frac{i}{kA}\left(\Omega\frac{\lambda+\mu}{k} - \omega_e\right)(h_1\, e^{\Lambda}\Omega^2\omega_e + h_2\, kp_2) + ih_2 \frac{\Omega^3}{k\omega_e} e^{-\Lambda}, \tag{43}$$

https://doi.org/10.1017/S002237789700576X Published online by Cambridge University Press

where we have taken $p = h_1 p_1 + h_2 p_2$, with h_1 and h_2 being the constants of integration. Requiring the RF potential to vanish at the cathode, $\phi_1(y = 0) = 0$, gives

$$(\Omega^2 - \omega^2)\, h_2 = \left(\frac{\Delta_0^2}{\Omega} - \omega \frac{\lambda_0 + \mu_0}{k}\right) h_1\, \omega, \tag{44}$$

where λ_0 and μ_0 are the values of the respective quantities at the cathode, $y = 0$. At the anode, the x component of the RF electric field is

$$\begin{aligned} E_{xa} &= -ik\phi_1(y = l)\, e^{\gamma t} \\ &= \frac{1}{kA}\left(\Omega - \omega_{ea} \frac{\lambda_a + \mu_a}{k}\right)(h_1\, e^{\Lambda_a} \Omega^2 \omega_{ea} + h_2\, k p_{2a})\, e^{\gamma t} - h_2 \frac{\Omega^2}{k} e^{-\Lambda_a} e^{\gamma t}, \end{aligned} \tag{45}$$

where the subscript a indicates that the appropriate quantity is to be evaluated at the anode.

This has now determined the WKB solutions of the RF problem. We have the boundary condition at the cathode set with (44), and the amplitude of the RF fields are determined by the x component of the RF electric field at the tip of the vanes, E_{xa}, by (45). Thus these two conditions will determine the constants h_1 and h_2, once E_{xa} is given. Next we match this RF solution of the plasma region to the RF fields in the slow-wave structure. From this, we can determine the linear RF growth rate, γ (the imaginary part of the RF frequency ω).

4. Matching to the slow-wave structure

The slow-wave structure is a waveguide, along with an electromagnetic RF wave can propagate. In the absence of a plasma, it has a dispersion relation $\omega_{a0}(k)$ that defines the modes that can propagate along it. In the presence of a plasma, this dispersion relation is distorted to varying degrees, depending on how the plasma interacts with the fringe field of the RF wave propagating in the structure. Since we are assuming that the plasma never penetrates into the slow-wave structure, we shall take the region inside the structure to always be a vacuum region. Therefore, inside this region, using Maxwell's equations, we could solve for the electromagnetic fields inside the structure, from which we can determine the fields along the tips of the vanes. In particular, at the tip of the vanes, there will be a definite value for the ratio of the averaged x and y components of the RF electric field. (The overall magnitude of these fields will be determined by the power level of the RF field in the slow-wave structure.) These are the values that we must match to the RF plasma solution.

For simplicity, we shall take the slow-wave structure to be a simple comb structure as shown in Fig. 1. The dispersion relation for this structure can be approximated by the following form (Salter 1959; Davidson *et al.* 1991). We take the width of the vanes to be a, the period from one vane to the next to be L and the depth of the vane to be s. Then it is easy to show that, for this structure, the average of the ratio of the x and y components of the electric field, at the tips of the vanes, will be

$$\frac{k\phi_{1a}}{\partial_y \phi_{1a}} = \frac{4 \sin^2(\frac{1}{2}ak)}{a^2 k^3 L} \frac{a\omega}{c} \tan\left(\frac{s\omega}{c}\right), \tag{46}$$

https://doi.org/10.1017/S002237789700576X Published online by Cambridge University Press

where c is the speed of light. For comparison, we note that in the absence of a plasma, this ratio can be determined from the vacuum values for the RF electric field in the empty cathode–anode region. In this case, we have (Slater 1959)

$$\left(\frac{k\phi_{1a}}{\partial_y \phi_{1a}}\right)_{ct} = \frac{\kappa}{k}\tanh(kl), \tag{47}$$

where $\kappa = (k^2 - \omega^2/c^2)^{1/2}$ and the subscript ct indicates the value in the absence of a plasma.

Evaluating (42) and (43) at the anode (tips of the vanes, $y = l$), using (44) to determine the ratio h_1/h_2, then, by (46), we could obtain a solution for the dispersion relation $\omega_a(k)$ of the combined plasma/slow-wave-structure combination. Obviously, it is too complex to solve analytically. However, all that is required at the moment is the linear growth rate of this RF mode. That we can obtain in an approximate manner as follows. The irregular solution p_2 has a singularity for real ω and k at the diocotron resonance $\omega_e = 0$. Thus, to have a well-defined solution, we must allow one or the other to become complex. We shall take k to be real and let ω have a small imaginary part. The solution p_2 will then become complex in general. We estimate its imaginary part as follows. First, we perform an integration by parts:

$$\int_0^y \frac{kA}{\omega_e^2} e^{-2\Lambda}\, dy = -\frac{kA}{\omega_e' \omega_e} e^{-2\Lambda}\Big|_0^y + \int_0^y \frac{k\, dy}{\omega_e} \frac{d}{dy}\left(\frac{A e^{-2\Lambda}}{\omega_e'}\right). \tag{48}$$

Recall that $\omega_e' = -kn_0/\Omega$. The first term on the right-hand side, as a function of y, will only have a significant imaginary part near the resonance. Away from the resonance, it will essentially become purely real. The second term, the integral, now has a simple pole at the resonance, since the derivative under the integral is non-singular. Let y_r designate the position of the resonance $\Re[\omega_e(y_r)] = 0$. When $y < y_r$, this integral is also essentially real. When $y > y_r$, in integrating across the resonance, this integral collects an imaginary part. Taking the imaginary part of (48) to be $Z(y)$, we find

$$\begin{aligned} Z(y) &\equiv \Im\left[\int_0^y \frac{kA}{\omega_e^2} e^{-2\Lambda}\, dy\right] \\ &\approx -\operatorname{sgn}(\gamma)\left[\frac{\pi k}{\omega_e'} \frac{d}{dy}\left(\frac{A e^{-\Lambda-\Lambda^*}}{\omega_e'}\right)\right]\Bigg|_{y=y_r} \theta(y - y_r) \\ &\approx \operatorname{sgn}(\gamma) \frac{\pi \Omega^4 n_{0r}'}{k n_{0r}^3} e^{-\Lambda_r - \Lambda_r'} \theta(y - y_r), \end{aligned} \tag{49}$$

where the subscripts r indicate the values at the resonance $y = y_r$, $\Im$ indicates the imaginary part, $\operatorname{sgn}(z)$ is the sign function and $\theta(z)$ is the Heaviside function.

Now, from (40), (42), (43) and (49), assuming that the imaginary part is small, so that h_2 and E_{ya} may be taken to be real, we obtain for the RF plasma mode

$$\Im\left[\frac{k\phi_{1a}}{\partial_y \phi_{1a}}\right] \approx -\frac{h_2^2 \Omega^4}{k E_{ya}^2} Z(l), \tag{50}$$

https://doi.org/10.1017/S002237789700576X Published online by Cambridge University Press

where E_{ya} is the y component of the RF electric field at the tips of the anode. Taking the expression for the same of the slow-wave structure, (46), we have

$$\Im\left[\frac{k\phi_{1a}}{\partial_y \phi_{1a}}\right] \approx \frac{k\phi_{1a}}{\partial_y \phi_{1a}} \frac{\gamma}{\omega} \sigma, \tag{51}$$

where σ is a characteristic parameter of the slow-wave structure (the logarithmic derivative of (46) with respect to ω), which, for the comb model, is given by

$$\sigma = 1 + \frac{2s\omega/c}{\sin(2s\omega/c)}. \tag{52}$$

Equating (50) and (51) and solving for γ gives

$$\gamma = \frac{h_2^2 \omega \Omega^4 Z(l)}{k\sigma E_{xa}(iE_{ya})}. \tag{53}$$

We now have all the RF quantities and parameters detailed that we shall need. Next we use these to analyse the second-order, or quasilinear, part of the plasma response.

5. Steady-state quasilinear solutions

We may now construct the quasilinear diffusion coefficient. From (19), (37) and (40), we have

$$D(y) = \frac{2\gamma\Omega^4}{k^2 A^* A} e^{2\Lambda} e^{2\gamma t} \left| h_1 + h_2 \int_0^y \frac{kA}{\omega_e^2} e^{-\Lambda - \Lambda^*} dy \right|^2, \tag{54}$$

assuming that there is only one RF mode present. Obviously, from (54), given ω, k, Ω, l, σ and $n_0(y)$, it is possible to calculate $D(y)$. However, $n_0(y)$ is itself given in terms of $D(y)$, (26), so this becomes a circuitous definition. But, as we have already discussed, we can expect a consistent solution to exist. How this could be obtained remains to be seen. It could well be that consistent solutions can only exist for a range of applied DC voltages, which could explain why these devices operate in a limited DC voltage range. At the moment, that is only speculation.

On the other hand, there is more information that can be obtained from (54) as it stands. Let us consider this expression at the resonance point $y = y_r$. Here, the integral in (54) could be approximated, since that is where the denominator in the integral is the smallest. Then, turning to (48), we see that the value of the integral at the resonance can be evaluated using only the first term. Thus, for $|\gamma| \ll |\omega|$, we find

$$\int_0^{y_r} \frac{kA}{\omega_e^2} e^{-2\Lambda} dy \approx -\frac{i\Omega^3}{n_{0r}\gamma} e^{-2\Lambda_r}. \tag{55}$$

Then, providing that the ratio h_2/h_1 is not too small, from (54) and (55),

$$D_r \equiv D(y = y_r) \approx \frac{2\Omega^6 |h_2|^2}{\gamma k^2 n_{0r}^2} e^{-\Lambda_r - \Lambda_r^*} e^{2\gamma t}, \tag{56}$$

showing that the quasilinear diffusion coefficient, at the resonance, is inversely

https://doi.org/10.1017/S002237789700576X Published online by Cambridge University Press

proportional to the diocotron growth rate γ. Contrast this with (54), where in other regions, the diffusion coefficient is directly proportional to the same.

Now, let us return to the expression for the diocotron growth rate. From (49) and (53), taking γ to be positive, we have

$$\gamma = \frac{\pi h_2^2 \Omega^8 \omega(-n_{0r}')\, e^{2\gamma t}}{k^2 \sigma n_{0r}^3 (-iE_{xa} E_{ya})} e^{-\Lambda_r - \Lambda_r^*}. \tag{57}$$

Of course, for the above solution to be valid, we have to have $(-iE_{xa}E_{ya})/h_2^2$ positive. We shall return to this point later. Combining (56) and (57), we have

$$D_r(-\partial_y n_0)_r \approx \frac{2\sigma n_{0r}}{\pi\omega\Omega^2}\left(-i\frac{h_2^*}{h_2}E_{xa}E_{ya}\right), \tag{58}$$

which, from (18), for the steady-state solutions and from the result (23) for the particle flux, gives

$$\begin{aligned} J_{2y} &= C_2 \Omega^2 \\ &= \frac{\Omega^2}{\Omega^2 - n_{0r}} D_r(-\partial_y n_0)_r \\ &\approx \frac{2\sigma n_{0r}}{\pi\omega(\Omega^2 - n_{0r})}\left(-i\frac{h_2^*}{h_2}E_{xa}E_{ya}\right). \end{aligned} \tag{59}$$

Let us now look at the phases of the electric field and h_2 and how they relate to the sign of γ. First, there is an overall arbitrary phase in the solutions for the RF wave. This phase can be fixed by choosing the phase of E_{xa} in (45). If we choose this phase to be purely imaginary then ϕ_1, p_1, p_2, h_1 and h_2 are mainly real, since we have assumed the imaginary parts to be small. Then we have

$$-i\frac{h_2^*}{h_2}E_{xa}E_{ya} = k\phi_{1a}(\partial_y \phi_1)_a\, e^{2\gamma t} \tag{60}$$

real. In order to have it also positive, which is required for the current J_{2y} (and γ in (57)) to be positive, the product of $\phi_1 \partial_y \phi_1$ at the anode must be positive. This is the usual case, since, as one approaches the vane tips from the plasma, ϕ_1 will increase.

6. Conclusions

One of the more surprising features of this result is the fact that no RF mode besides the existence of an RF signal in the slow-wave structure has been required. We have only assumed that the RF signal in the slow-wave structure drives the plasma response. In other words, no resonant plasma mode has been required. This is not to say that one would not exist. Rather, it is not needed in order for a CFA to draw current. The dynamics of the plasma response seem to be governed only by the properties of the slow-wave structure. This immediately brings into question whether or not anything such as a 'resonant diocotron plasma mode' does exist. Almost all previous work has centred on attempting to find such a mode (Beuneman *et al.* 1966; Loveland and Ott 1974; Swegle and Ott 1981; Swegle 1983; Kaup and Thomas 1992*a*, 1996), which

https://doi.org/10.1017/S002237789700576X Published online by Cambridge University Press

could exist under smooth bore conditions ($\phi_a = 0$). Naturally, if it does exist, then one would have to include it in the analysis also, since it would then be expected to resonant with the above mode, driven by the RF signal in the slow-wave structure (which was called the 'anode mode' in Kaup and Thomas 1996). However, before one can determine if such a 'resonant diocotron plasma mode' exists, one would first have to have solutions for the steady-state background density profile, since such a mode would have to exist on this background.

Clearly the result given by (60) shows that the DC current drawn by a device will be directly proportional to the power propagating through the slow-wave structure. However, until one knows the propagation constant for the slow-wave structure, one cannot predict numerical values, since the power flow is proportional to this factor. However, if one knew the values of the electric field strengths at the vane tips, the value of the propagation constant and the electron density at the diocotron resonance, then (60) would provide a means for determining the DC current in a device.

One more feature of (26) that should be noted is the fact that it predicts that the steady-state density profile will be independent of the current and the power delivered. Although D is proportional to the RF power, so is C_2. Thus the density profile given by (26) will be unchanged if one changes the DC current. This in turn implies that it is the ability of the cathode to deliver electrons into the cathode–anode spacing that will limit the gain of such a crossed-field device.

Acknowledgements

This research was supported in part by the Air Force Office of Scientific Research, under Grant F49620-93-1-0088, and the Naval Surface Warfare Center, Crane Division.

References

Antonsen, T. M., Ott, E., Chang, C. L. and Drobot, A. T. 1985 *Phys. Fluids* **28**, 2878.

Brillouin, L. 1945 *Phys. Rev.* **67**, 260.

Buneman, O., Levy, R. H. and Linson, L. M. 1966 *J. Appl. Phys.* **37**, 3203.

Chan, H.-W., Chen, C. and Davidson, R. C. 1993 *J. Appl. Phys.* **73**, 7053.

Christenson, P. J. and Lau, Y. Y. 1994 *Phys. Plasmas* **1**, 3725.

Church, B. W. and Sudan, R. N. 1995 *Phys. Plasmas* **2**, 1837.

Davidson, R. C. 1984 *Phys. Fluids* **27**, 1804.

Davidson, R. C. 1985*a* *Phys. Fluids* **28**, 377.

Davidson, R. C. 1985*b* *Phys. Fluids* **28**, 1937.

Davidson, R. C. and Tang, K. T. 1985 *Phys. Fluids* **28**, 1169.

Davidson, R. C., Tang, K. T. and Swegle, J. A. 1984 *Phys. Fluids* **27**, 2332.

Davidson, R. C., Tang, K. T. and Uhm, H. S. 1988 *Phys. Fluids* **37**, 1727.

Davidson, R. C., Chan, H.-W., Chen, C. and Lund, S. 1991 *Rev. Mod. Phys.* **63**, 341.

Desjarlais, M. P. and Sudan, R. N. 1986 *Phys. Fluids* **29**, 1245.

Desjarlais, M. P. and Sudan, R. N. 1987 *Phys. Fluids* **30**, 1536.

Drazin, P. G. and Reid, W. H. 1981 *Hydrodynamic Stability*, Chap. 4. Cambridge University Press.

Jablonski, M. K. 1992 A Comparison of linear perturbation analysis with computer simulation results for a planar magnetron. MSc thesis, MIT.

Kaup, D. J. and Thomas, G. E. 1988 *Phys. Fluids* **31**, 2362.

Kaup, D. J. and Thomas, G. E. 1989 *Stud. Appl. Maths* **81**, 37 [*Erratum* **83**, 271 (E) (1990)].

https://doi.org/10.1017/S002237789700576X Published online by Cambridge University Press

Kaup, D. J. and Thomas, G. E. 1992*a* *J. Appl. Phys.* **71**, 5752.

Kaup, D. J. and Thomas, G. E. 1992*b* *Phys. Fluids* **B4**, 2640.

Kaup, D. J. and Thomas, G. E. 1996 *Phys. Plasmas* **3**, 771.

Lau, Y. Y. and Chernin, D. 1992 *Phys. Fluids* **B4**, 3473.

Lau, Y. Y., Christenson, P. J. and Cherin, D. 1993 *Phys. Fluids* **B5**, 4486.

Loveland, R. V. and Ott, E. 1974 *Phys. Fluids* **17**, 1263.

MacGregor, R., Chan, C., Ye, J. Z. and Ruden, T. E. 1994 *IEEE Trans. Electron Devices* **41**, 1456.

Prasad, S. A., Morales, G. J. and Fried, B. D. 1987 *Phys. Fluids* **30**, 3093.

Riyopoulos, S. 1996 *Phys. Plasmas* **3**, 1137.

Slater, J. C. 1959 *Microwave Electronics*, Chap. 13. Van Nostrand, Princeton.

Swegle, J. 1983 *Phys. Fluids* **26**, 1670.

Swegle, J. and Ott, E. 1981 *Phys. Fluids* **24**, 1821.

Uhm, H. S. 1992 *Phys. Fluids* **B4**, 740.

Ye, J. Z., Chan, C., MacGregor, R. and Ruden, T. E. 1994 *IEEE Trans. Electron Devices* **41**, 258.

https://doi.org/10.1017/S002237789700576X Published online by Cambridge University Press